Scientific Visualization, 2020, volume 12, number 4, pages 108 - 122, DOI: 10.26583/sv.12.4.10

Stress-strain state interactive visualization of the parametrically-defined thin-shell structures with the use of AR and VR technologies

A.A. Semenov[1], Iu.N. Zgoda[2]

Saint Petersburg State University of Architecture and Civil Engineering, Saint-Petersburg

[1] ORCID: 0000-0001-9490-7364, sw.semenov@gmail.com
[2] ORCID: 0000-0001-6714-500X, yurii.zgoda@mail.ru

Abstract

The paper describes a mathematical model of changes in the geometry of thin-shell structures for visualization of the analysis data on their stress-strain state (SSS).

Based on this mathematical model, a module for shell SSS visualization using VR and AR technologies was developed. The interactive visualization environment Unity 2019.3 and C# programming language were used. The interactive visualization module makes a 3D image of a shell structure and visualizes the SSS either through heat maps over the shell or through the changes in the shell geometry via the shell type, its geometric characteristics, and SSS analysis data (transferred to the visualization module by means of a JSON file).

While working on the visualization module, the authors developed a software system that makes it possible to visualize any 3D surface with coordinate axes (including numbers with a pitch determined automatically), visualize heat maps with a graduated scale, visualize a mesh over the graph to improve the perception of the surface deformations. The middle surface deformation can also performed via SSS analysis data.

This solution increases the efficiency of the work of specialists in civil engineering and architecture and can be used when training specialists in courses on thin-shell structures and procedural geometry.

Keywords: shells, stress-strain state, virtual reality, augmented realty, parametric modeling, Ritz method, Unity.

1. Introduction

Thin-shell structure (or shell) is a body bounded by two curved surfaces, the greatest distance between which is much less than any other size. (Fig. 1). Great attention is paid to studies on shells since such structures are highly strong and stiff and have a variety of design shapes [1], [2]. Thin-shell structures are often used in shipbuilding, aircraft and spacecraft construction, mechanical and civil engineering.

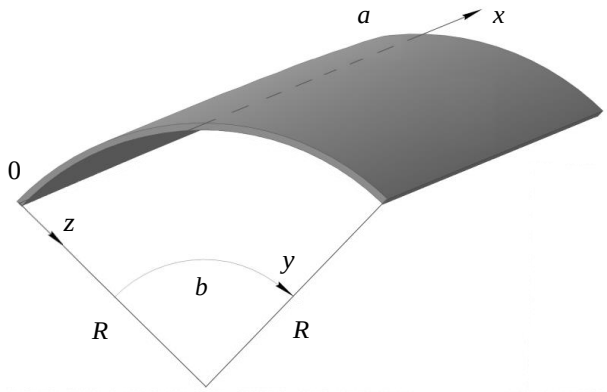

Fig. 1. Thin-walled shell structure

During operation shell structures are subjected to various influences (mechanical static loads, vibrations, shock loads, temperature effects, etc.) and can also exhibit various properties (loss of stability, plastic deformation, material creep, etc.). Thereat, a wide class of problems arises that require research. The capabilities of modern computer hardware make it possible to perform calculations with high accuracy and consideration of complex nonlinear effects.
The current state of different shell theory branches be found in review articles [3-8].
Although the visualization of complex engineering processes is very important [9], the issues of shell visualization have not been solved in full. The research on shells often covers only the stress-strain state (hereinafter — the SSS) of a shell structure relative to the middle surface (Fig. 2), while deformations in the global coordinates are not considered. The middle surface of a shell is the locus of points equidistant from the two surfaces that form this shell. Although such software packages as ANSYS and LIRA-SAPR enable graphic visualization of deformations, there is no standard technique or algorithm of visualization of deformed shells for variational analysis methods which are widely used in shell modeling [10-12]. In the meantime, the use of variational methods such as the Ritz method can significantly improve the accuracy of the analysis and reduce its time [2].

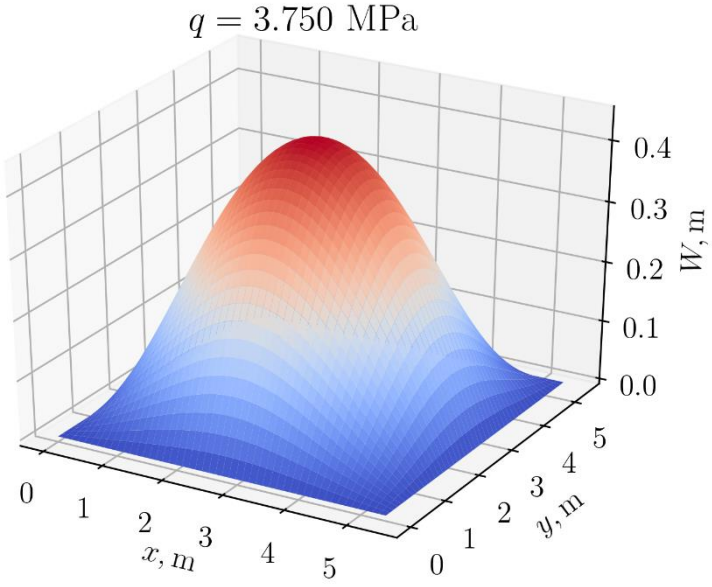

Fig. 2. Visualization of vertical displacements relative to the middle surface

Informative visualization of the SSS of shells is important for their detailed study [13]. In many cases, a researcher will examine the analysis data more efficiently if they are presented as a 3D animation rather than static contoured maps or 2D graphs. For example, using the shell structure's stress-strain state 3D visualization it is possible to verify the results of calculations with field experiments [14].
VR and AR technologies are particularly important in this context [15, 16]. Virtual reality gives a 3D representation of structural deformations. This allows visualizing the change in shell geometry more accurately relatively to its original dimensions. Augmented reality makes it possible to see the structure in the real world, which is also useful for studies on shell structures. For example, augmented reality allows visualizeing the 3D-model of the deformed shell on top of a paper report of its SSS study. This provides theo significant increase in the information on used documentation tools.
The purpose of this study is to develop a software package (hereinafter — the SP) for the analysis of the SSS and visualization of shell structures using VR and AR technologies. To achieve this purpose, different problems were solved:
A mathematical model of the thin-shell structure geometric data was formed. This model defines shell geometry in the global coordinate system and allows the addition of deformation data obtained during SSS calculation.
A software package has been implemented that generates geometry based on the calculation results. It allows visualizing various fields of SSS and provides standard elements for visualizing 3D graphs (such as coordinate axes and heat maps).

2. SP Architecture

The software package consists of two modules: the SSS analysis module and the visualization module. The SP architecture is shown in Fig. 3.
The analysis module performs shell structure SSS analysis that is based on the functional of the total strain energy using GPU. The Ritz method [2] is used for the numerical solution of the variational problem. This method reduces the problem of minimizing the functional to the problem of minimizing the function of multiple variables. The results of the SSS analysis that fully describe the deformation of the shell structure in all its points are the coefficients of approximation functions that provide the functional minimum. The analysis data can be exported by means of JSON files for subsequent visualization in the visualization module.

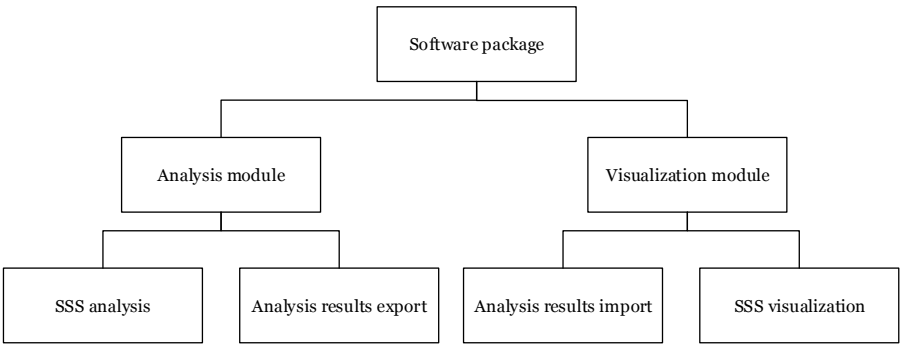

Fig. 3. Software package for shell analysis

The visualization module deserializes the file with the SSS analysis data, performs procedural generation of the geometry of the shell structure, and, then, visualizes the SSS through either heat maps presented over the shell or through changing the geometry of the shell structure.
The main feature of the described solution is the ability to render shell SSS using virtual and augmented reality technologies. Recently, there are no solutions that allow visualizing the calculation results stored in standard formats (such as VTK) on mobile augmented or virtual

reality platforms. For this reason, existing renderers (such as ParaView) couldn't be used and a custom rendering solution was developed. Visualization module imports the analysis results in custom data format used for SSS data storage in the analysis module because using other data formats doesn't provide benefits within the investigated problem.

3. SSS of a Shell

Analysis of the SSS of a shell structure means minimization of the functional of the total potential strain energy (which is a sum of the work of internal and external forces) in the Timoshenko (Reissner–Mindlin) model. The Ritz method is used for numerical search for the functional minimum. It reduces the variational problem to a problem of unconstrained optimization of the function of several variables. For this purpose, the required displacements functions $U(x, y), V(x, y), W(x, y)$ as well as functions of normal segment turning angles to the middle surface $\Psi_x(x, y), \Psi_y(x, y)$ are replaced with the following approximations:

$$U = U(x,y) = \sum_{k=1}^{\sqrt{N}} \sum_{l=1}^{\sqrt{N}} U_{kl} X_1^k Y_1^l, \quad V = V(x,y) = \sum_{k=1}^{\sqrt{N}} \sum_{l=1}^{\sqrt{N}} V_{kl} X_2^k Y_2^l,$$

$$W = W(x,y) = \sum_{k=1}^{\sqrt{N}} \sum_{l=1}^{\sqrt{N}} W_{kl} X_3^k Y_3^l, \tag{1}$$

$$\Psi_x = \Psi_x(x,y) = \sum_{k=1}^{\sqrt{N}} \sum_{l=1}^{\sqrt{N}} PS_{kl} X_4^k Y_4^l, \quad \Psi_y = \Psi_y(x,y) = \sum_{k=1}^{\sqrt{N}} \sum_{l=1}^{\sqrt{N}} PN_{kl} X_5^k Y_5^l,$$

where approximation functions $X_1^k - X_5^k, Y_1^l - Y_5^l$ are known and predetermined by the conditions of shell fixing, and parameters $U_{kl} - PN_{kl}$ are unknown numeric coefficients; N – is the quantity of expansion terms.

Thus, the functional $E_s = E_s(U, V, W, \Psi_x, \Psi_y)$ (complete expression is given in [2, 17]) is approximated by the function of several variables, and it is sufficient to use the approximation functions and the numeric coefficients' values ensuring the minimum of the functional to recover the SSS analysis data.

4. Geometry of a Shell

When using variational principles for making a mathematical model, the geometry of a shell structure is found through Lame parameters and principal curvatures. However, it does not seem too comfortable to make a curvilinear coordinate system to generate the geometry of a shell structure based on these parameters only. Papers dealing with shell visualization [18] suggest using a parametric notation for shell structures instead.

Many shells can be described in the parametric form, which relates each of the points of the middle surface in a 2D space to a point in a 3D coordinate system. Therefore, the question of how deformations are applied to the shell middle surface should be solved. In this paper, the local basis in each point of the middle surface is used to solve this problem, which makes it possible to use displacements in the global coordinates instead of displacements $U(x, y), V(x, y), W(x, y)$ relative to the middle surface. We build the geometry of a shell with a certain thickness h, ratios for displacements in an arbitrary layer of the shell from the Timoshenko model that is a base for the analysis for the middle surface.

Let us describe a parametric shell in a generalized form below. Each point of such a shell is determined through the following ratios:

$$\begin{cases} X = X(x, y), \\ Y = Y(x, y), \\ Z = Z(x, y). \end{cases} \quad (2)$$

To apply deformations, i.e. displacement of the points in a horizontal, vertical and normal directions, to such a geometry, we need to find vectors $N_U = \left(\frac{\partial X}{\partial x}, \frac{\partial Y}{\partial x}, \frac{\partial Z}{\partial x}\right)$, $N_V = \left(\frac{\partial X}{\partial y}, \frac{\partial Y}{\partial y}, \frac{\partial Z}{\partial y}\right)$ for each point of the shell, after which they should be normalized. These vectors determine the horizontal and vertical directions of displacement of the points, respectively. The vector product of these normalized vectors is the normal to the surface of the shell in the point $N_W(x, y)$. Sign of the normal vector is defined so that it shows the direction from the inside-out. Analytical expressions of the basis of these vectors are derived for various types of shell structures in this paper.

4.1. Doubly Curved Shallow Shell

The input parameters of a doubly curved shallow shell are linear dimensions a, b, and radii of circular arcs R_1, R_2. Let us introduce additional parameters $R = \max\{R_1, R_2\} - \min\{R_1, R_2\}$ and $r = \min\{R_1, R_2\}$. In this case, the parametric form for this shell will be as follows:

$$\begin{cases} X = (R + r\cos x)\sin y, \\ Y = (R + r\cos x)\cos y, \\ Z = r\sin x. \end{cases} \quad \begin{cases} x \in \left[-\frac{\min\{a,b\}}{2r}, \frac{\min\{a,b\}}{2r}\right], \\ y \in \left[-\frac{\max\{a,b\}}{2(R+r)}, \frac{\max\{a,b\}}{2(R+r)}\right], \end{cases} \quad (3)$$

where x is the turning angle of a small radius; y is the turning angle of a large radius.
The expression for the basis in each point of the shell is as follows:

$$\begin{cases} N_U = (-\sin x \sin y,\ -\sin x \cos y,\ \cos x), \\ N_V = (\cos y,\ -\sin y,\ 0), \\ N_W = (\cos x \sin y,\ \cos x \cos y,\ \sin x). \end{cases} \quad (4)$$

The middle surface of a shallow shell is given in Fig. 4.

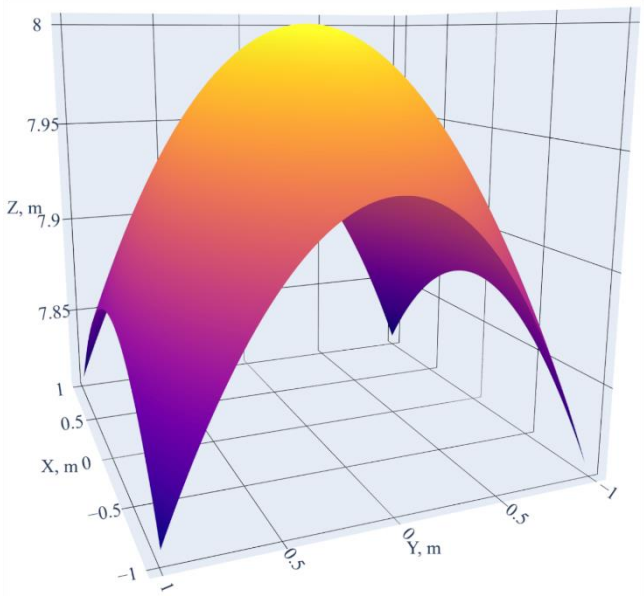

Fig. 4. Middle surface of a doubly curved shallow shell

4.2. Spherical Shell

The input parameters of a spherical shell are linear parameters a, a_1, b and radius R. The parametric form of a spherical shell is as follows:

$$\begin{cases} X = R\sin x\sin y, \\ Y = R\cos x, \\ Z = -R\sin x\cos y. \end{cases} \quad \begin{cases} x \in [a_1, a], \\ y \in \left[-\frac{b}{2}, \frac{b}{2}\right], \end{cases} \tag{5}$$

where x and y coincide with the latitude and longitude, respectively. The basis in the point of the middle surface is determined as follows:

$$\begin{cases} N_U = (\cos x\sin y,\ -\sin x,\ -\cos x\cos y), \\ N_V = (\cos y,\ 0,\ \sin y), \\ N_W = (\sin x\sin y,\ \cos x,\ -\sin x\cos y). \end{cases} \tag{6}$$

The appearance of the middle surface of a spherical shell is given in Fig. 5.

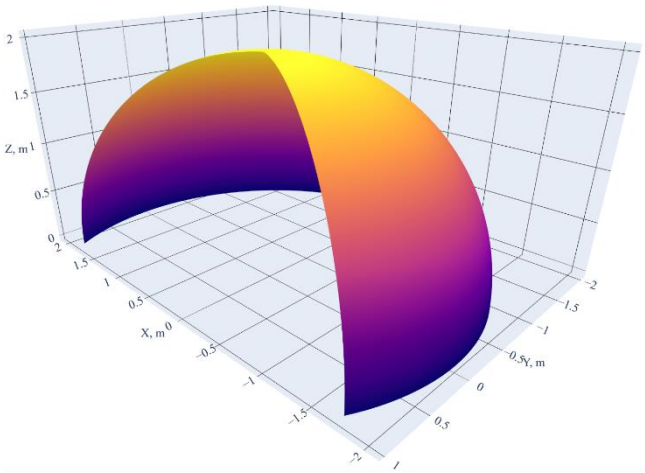

Fig. 5. Middle surface of a spherical shell

4.3. Toroid-Shape Shell

The model of a toroid-shape shell coincides with the model of a spherical shell but includes displacement d_1 from the vertical axis of rotation of the sphere. The parametric form of a toroid-shape shell is as follows:

$$\begin{cases} X = R\sin x\sin y + d_1\sin y, \\ Y = R\cos x, \\ Z = -R\sin x\cos y - d_1\cos y. \end{cases} \quad \begin{cases} x \in [a_1, a], \\ y \in \left[-\frac{b}{2}, \frac{b}{2}\right]. \end{cases} \tag{7}$$

The basis in the point of the middle surface is determined as follows:

$$\begin{cases} N_U = (\cos x\sin y,\ -\sin x,\ -\cos x\cos y), \\ N_V = (\cos y,\ 0,\ \sin y), \\ N_W = (\sin x\sin y,\ \cos x,\ -\sin x\cos y). \end{cases} \tag{8}$$

The appearance of the middle surface of a toroid-shape shell is given in Fig. 6.

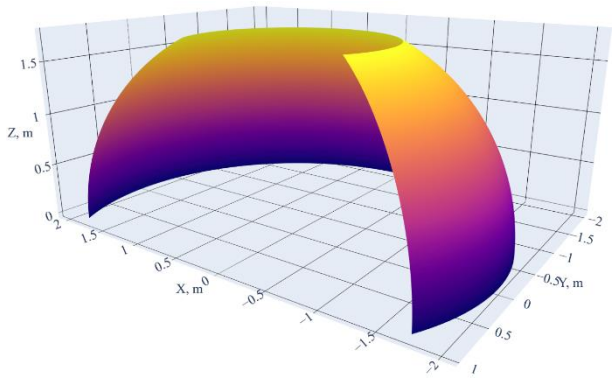

Fig. 6. Middle surface of a toroid-shape shell

4.4. Cylindrical Shell

The input parameters of a cylindrical shell are linear dimensions a, a_1, b and radius R. The parametric form of a cylindrical shell is as follows:

$$\begin{cases} X = x - \dfrac{a - a_1}{2}, \\ Y = R\cos y - R, \\ Z = -R\sin y. \end{cases} \quad \begin{cases} x \in [a_1, a], \\ y \in \left[-\dfrac{b}{2}, \dfrac{b}{2}\right]. \end{cases} \tag{9}$$

Curvilinear coordinate x is along the element, while curvilinear coordinate y is along the circle made by the cross-section of the cylinder with a plane parallel to its base.
The basis in an arbitrary point of the middle surface is as follows:

$$\begin{cases} N_U = (1,\ 0,\ 0), \\ N_V = (0,\ -\sin y,\ -\cos x), \\ N_W = (0,\ \cos y,\ -\sin y). \end{cases} \tag{10}$$

The appearance of the middle surface of a cylindrical shell is given in Fig. 7.

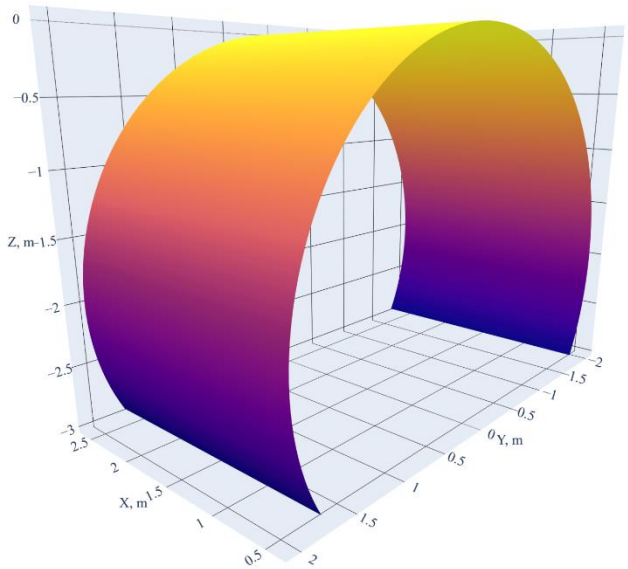

Fig. 7. Middle surface of a cylindrical shell

4.5. Catenoid Shell

The input parameters of a catenoid shell are linear dimensions a, a_1, b and parameter c. The parametric form of a catenoid shell is as follows:

$$\begin{cases} X = x - \dfrac{a - a_1}{2}, \\ Y = c \cdot \cosh\left(x - \dfrac{a - a_1}{2} \right) \cos y - c, \\ Z = -c \cdot \cosh\left(x - \dfrac{a - a_1}{2} \right) \sin y. \end{cases} \quad \begin{cases} x \in [a_1, a], \\ y \in \left[-\dfrac{b}{2}, \dfrac{b}{2} \right]. \end{cases} \tag{11}$$

The basis for such a shell takes the following form:

$$\begin{cases} N_U = \dfrac{\left(1,\ c\sinh\left(\dfrac{a - a_1}{2} - x \right) \cos y,\ c\sinh\left(\dfrac{a - a_1}{2} - x \right) \sin y \right)}{\sqrt{c^2 \sinh^2\left(x - \dfrac{a_1 - a}{2} \right) + 1}}, \\ N_V = (0,\ -\sin y,\ -\cos y), \\ N_W = \dfrac{\left(c\sinh\left(\dfrac{a - a_1}{2} - x \right),\ \cos y,\ -\sin y \right)}{\sqrt{c^2 \sinh^2\left(\dfrac{a_1 - a}{2} - x \right) + 1}}. \end{cases} \tag{12}$$

The appearance of the middle surface of a catenoid shell is given in Fig. 8.

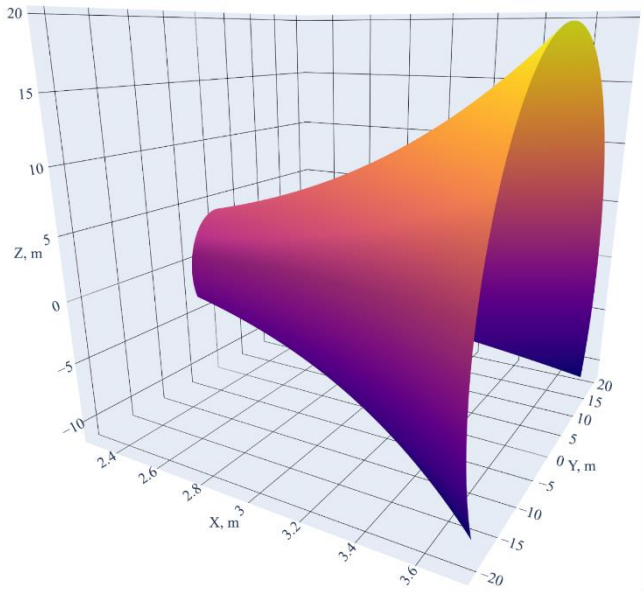

Fig. 8. Middle surface of a catenoid shell

4.6. Conical Shell

The input parameters of a conical shell are linear dimensions a, a_1, b. The parametric form of a conical shell is as follows:

$$\begin{cases} X = x\cos\theta - \dfrac{a_1 + a}{2}, \\ Y = x\sin\theta\cos y, \\ Z = -x\sin\theta\sin y. \end{cases} \quad \begin{cases} x \in [a_1, a], \\ y \in \left[-\dfrac{b}{2}, \dfrac{b}{2} \right]. \end{cases} \tag{13}$$

Curvilinear coordinate x is along the element, while curvilinear coordinate y is along the circle made by the cross-section of the cone with a plane parallel to its base.

The basis for a conical shell is as follows:

$$\begin{cases} N_U = (\cos\theta,\ \sin\theta\cos y,\ -\sin\theta\sin y), \\ N_V = (0,\ -\sin y,\ -\cos y), \\ N_W = (-\sin(\theta),\ \cos y\cos\theta,\ -\cos\theta\sin y). \end{cases} \quad (14)$$

The appearance of the middle surface of a conical shell is given in Fig. 9.

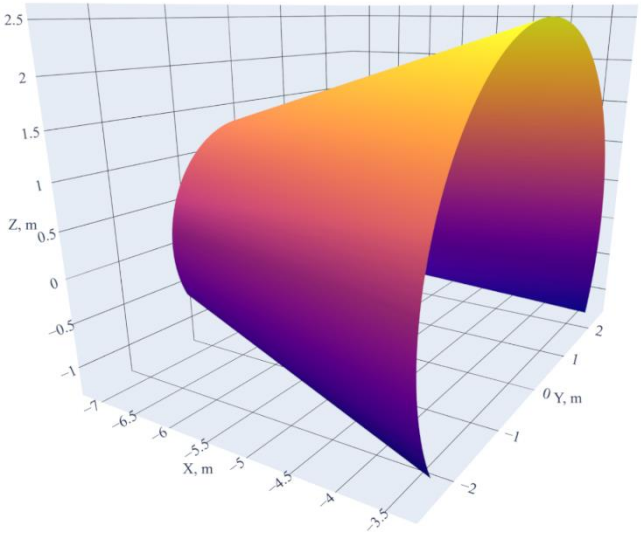

Fig. 9. Middle surface of a conical shell

5. Deformed shell geometry

After the determination of shell's middle surface parametric form and it's local basis at each point, it is possible to build a deformed structure in the global coordinate system.

Let M_0 be a point of shell's middle surface. Then the coordinates of this point after shell loading and the following deformation M_D is defined as follows:

$$M_D = M_0 + N_U U + N_V V - N_W W, \quad (15)$$

where the negative sign in front of the term responsible for the vertical component of deformation is due to the positive direction of the shell deflection.

Formula (15) allows constructing the deformed geometry of shell's middle surface. In order to move from middle surface to bulk body, it is necessary to determine how various layers of shell are deformed.

According to Timoshenko-Reisner model, during deformation a rectilinear shell element, initially normal to middle surface, remains rectilinear, but not necessarily normal. In this case, the displacements in the layer spaced z from the middle surface have the form:

$$U^z = U + z\Psi_x, \quad V^z = V + z\Psi_y, \quad W^z = W, \quad (16)$$

where Ψ_x, Ψ_y are the rotation angles of segment normal to the middle surface in sections $x0z$ and $y0z$ respectively. Fig. 10 shows the results of shell visualization with zero thickness (i.e, visualization of the middle surface) and with thickness equal to 0.09 m.

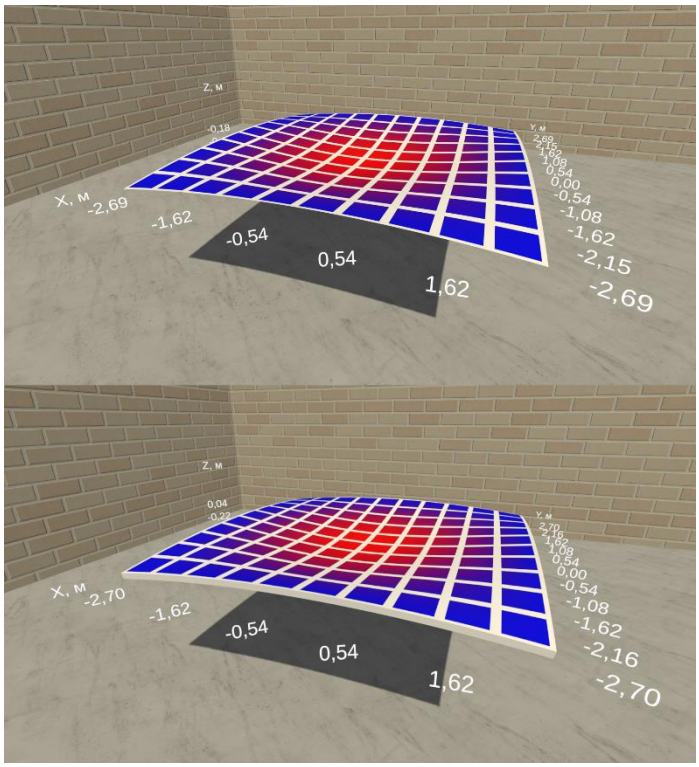

Fig. 10. Shell visualization with zero thickness (top) and with thickness equal to 0.09 m (bottom).

6. Shell Visualization

To implement the shell visualization module that uses VR and AR technologies, the interactive visualization environment Unity 2019.3 and C# programming language were used. The interactive visualization module makes a 3D image of a shell structure and visualizes the SSS either through heat maps over the shell or through the changes in the shell geometry that depend on the shell type, its geometric characteristics, and SSS analysis data (transferred to the visualization module by means of a JSON file).

In order to generate geometry for different types of shells, the following software architecture is proposed. The logic associated with procedural mesh generation is located in abstract class ShellGeometryGenerator. This class includes methods for generating bulk body's mesh, considering it's SSS. Child classes of this abstract class must implement methods that describe the middle surface of the shell parametrically. Thus, to visualize any type of shell construction not considered in this work, it is sufficient to describe its parametric form.

While working on the visualization module, the authors developed a system of components that makes it possible to visualize any 3D surface with coordinate axes (including numbers with a pitch determined automatically), visualize heat maps with a graduated scale, visualize a mesh over the graph to improve the perception of the surface deformations. The middle surface can also be deformed via SSS analysis data.

There is an option of using the proposed module without SSS visualization. This visualization mode can be useful to architects when they examine various forms of structures and to students studying shell structures. This allows for a better understanding of a relationship between the parameters of a shell structure and its final appearance.

Visualization module supports virtual reality devices Oculus Rift, HTC Vive, etc.), mobile virtual reality devices (Oculus Quest) and Android mobile devices that support ARCore technology.

7. Results and Discussion

The SP for visualization of shell structures was tested for shells of various shapes and using various visualization options. Fig. 11 provides a demonstration of the SSS of a shell structure using heat maps and geometry changes.

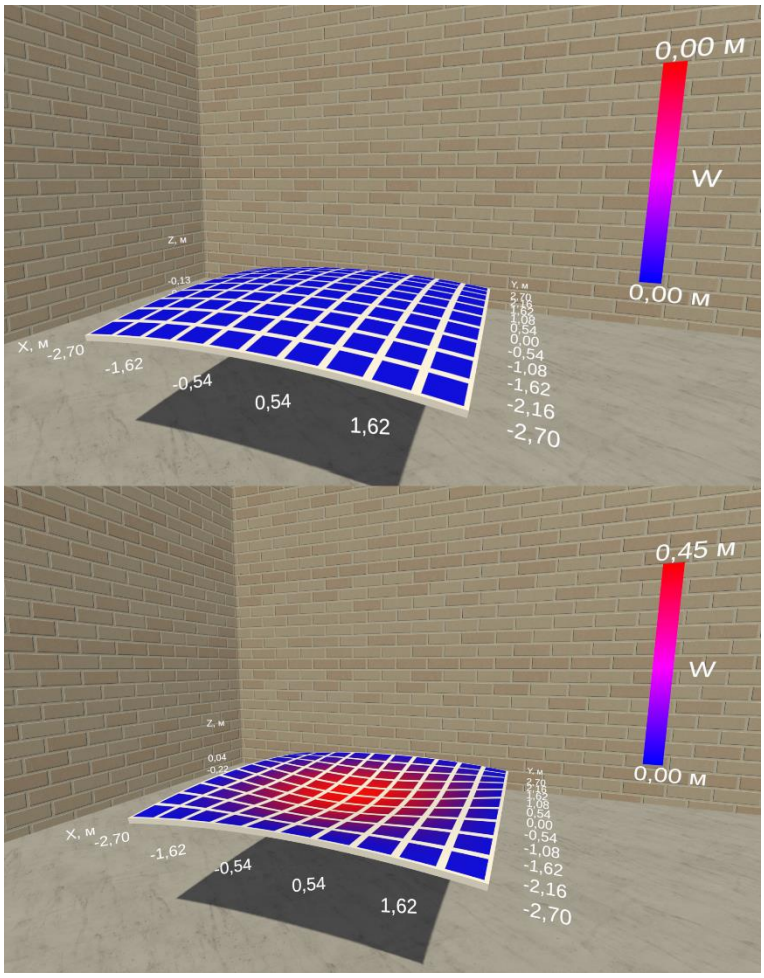

Fig. 11. Shell before (top) and after (bottom) applying the load

As follows from Fig. 11, visualization has great information capacity and describes data on the shell deformation both visually and numerically. The suggested visualization module helps to study the shell SSS in real-world scale with the initial proportions preserved. The clarity of such visualization in comparison to traditional visualization of the deflection relative to the middle surface (Fig. 2) is obvious.

As stated above, the suggested visualization module not only makes it possible to visualize the shell SSS but also can be used by students studying procedural modeling in architecture allowing them to clearly depict shell structures depending on their geometric parameters. Fig. 12 presents a shallow shell with lesser curvature radii and larger linear dimensions than those in Fig. 10. As you can see, a change in geometric parameters of shells of the same type can lead to significant changes in the final shape.

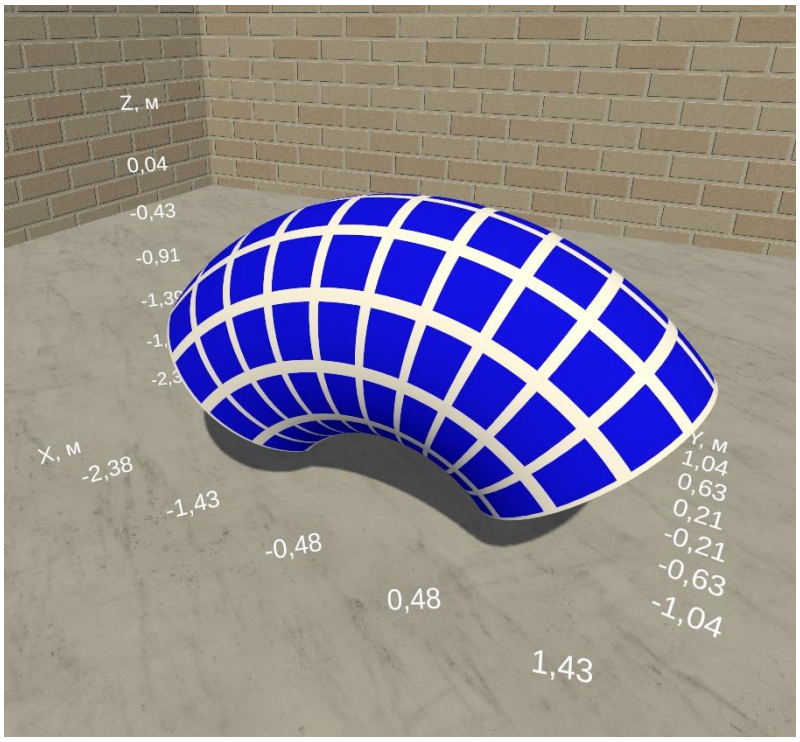

Fig. 12. Visualization of a shell with a small radius of rotation

The visualization module implements VR and AR technologies. AR visualization is demonstrated in Fig. 13. Such visualization can be used in cases where it is required to visually demonstrate the coincidence or non-coincidence between physical and mathematical modeling results. Also, augmented reality visualization can be used in the preparation of textbooks or reports on the study of shell SSS.

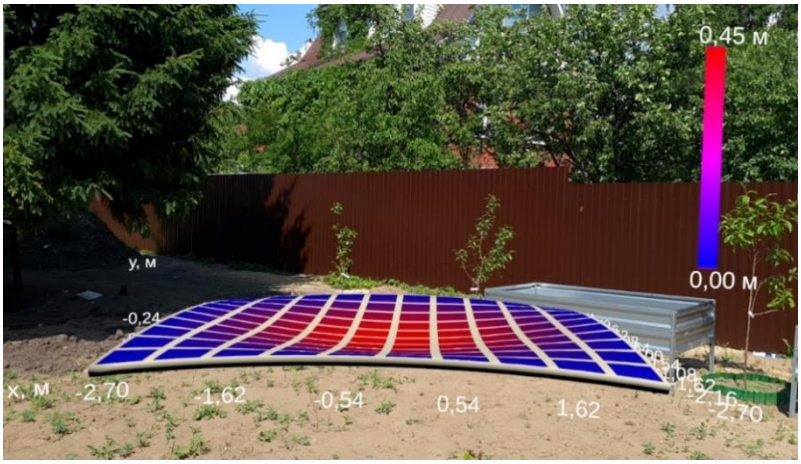

Fig. 13. AR visualization of a shell

It is planned to extend the functionality of the developed SC in the following directions:

- Allowing the user to define more complex types of shells, such as cutout shells.
- Implementing more accurate deformation models in different layers of the shell.
- Extending functionality of the SC (implementation of interactive cursors, three-dimensional grid graphics, etc.).

8. Conclusion

Thus, a mathematical model was developed that allows visualization of the SSS of shell structure determined by solving the variational problem. This mathematical model is implemented in the form of cross-platform software complex which allows the visualization of SSS with the use of virtual and augmented reality technologies. Currently, there are no other works describing the visualization of shell SSS by using these technologies.

The developed solution can be used as a tool for informative and clear visualization of the shell SSS, as a documenting tool or when training students majoring in architecture and civil engineering in courses on thin-shell structures.

Acknowledgments

The research was supported by RSF (project No. 18-19-00474).

References

1. Solovei N.A., Krivenko O.P., Malygina O.A.: Finite element models for the analysis of nonlinear deformation of shells stepwise-variable thickness with holes, channels and cavities // Magazine of Civil Engineering, Vol. 53, № 1, 2015, pp. 56–69 (doi:10.5862/MCE.53.6) (https://engstroy.spbstu.ru/en/article/2015.53.6/)
2. Karpov V.V.: Strength and stability of reinforced shells of rotation. In two parts. Part 1. Models and algorithms for studying the strength and stability of reinforced shells of rotation // Fizmatlit, Moscow, 2010.
3. Godoy L. A. Buckling of vertical oil storage steel tanks: Review of static buckling studies // Thin-Walled Structures. Vol. 103, 2016, pp. 1–21 (doi:10.1016/j.tws.2016.01.026) (https://www.sciencedirect.com/science/article/abs/pii/S026382311630026X)
4. Kumar P., Srinivasa C. On buckling and free vibration studies of sandwich plates and cylindrical shells: A review // Journal of Thermoplastic Composite Materials. Vol. 33, № 5, 2020, pp. 673–724 (doi:10.1177/0892705718809810) (https://journals.sagepub.com/doi/10.1177/0892705718809810)
5. Qatu M. S., Asadi E., Wang W. Review of Recent Literature on Static Analyses of Composite Shells: 2000-2010 // Open Journal of Composite Materials. Vol. 2, № 3. 2012, pp. 61–86 (doi:10.4236/ojcm.2012.23009) (https://www.scirp.org/journal/paperinformation.aspx?paperid=21295)
6. Alijani F., Amabili M. Non-linear vibrations of shells: A literature review from 2003 to 2013 // International Journal of Non-Linear Mechanics. Vol. 58, 2014, pp. 233–257 (doi:10.1016/j.ijnonlinmec.2013.09.012) (https://www.sciencedirect.com/science/article/abs/pii/S0020746213001868).
7. Maksimyuk V. A., Storozhuk E. A., Chernyshenko I. S. Variational finite-difference methods in linear and nonlinear problems of the deformation of metallic and composite shells (review) // International Applied Mechanics, Vol. 48, № 6, 2012, pp. 613–687 (doi:10.1007/s10778-012-0544-8).
8. Thai H.-T., Kim S.-E. A review of theories for the modeling and analysis of functionally graded plates and shells // Composite Structures, Vol. 128, 2015, pp. 70–86. (doi:10.1016/j.compstruct.2015.03.010) (https://www.sciencedirect.com/science/article/pii/S0263822315001828).
9. Zheleznyakova E.A., Osintsev A.V. Determination natural frequencies and mode shapes imaging element structures. Scientific Visualization, Vol. 10, № 3, 2018, pp. 45–57 (doi:10.26583/sv.10.3.03) (http://sv-journal.org/2018-3/03/?lang=en)
10. Chai Y., Song Z., Li F. Investigations on the aerothermoelastic properties of composite laminated cylindrical shells with elastic boundaries in supersonic airflow based on the

Rayleigh–Ritz method. Aerospace Science and Technology, Vol. 82, 2018, pp. 534-544 (doi:10.1016/j.ast.2018.09.040) (https://www.sciencedirect.com/science/article/abs/pii/S1270963818306102)
11. Deng J., Guasch O., Maxit L., Zheng L. Vibration of cylindrical shells with embedded annular acoustic black holes using the Rayleigh-Ritz method with Gaussian basis functions. Mechanical Systems and Signal Processing, Vol. 150, 2021, 107225 (doi:10.1016/j.ymssp.2020.107225) (https://www.sciencedirect.com/science/article/abs/pii/S0888327020306117)
12. Senjanović I., Alujević N., Ćatipović I., Čakmak D., Vladimir N. Vibration analysis of rotating toroidal shell by the Rayleigh-Ritz method and Fourier series. Engineering Structures, Vol. 173, 2018, pp. 870-891 (doi:10.1016/j.engstruct.2018.07.029) (https://www.sciencedirect.com/science/article/abs/pii/S0141029617332534)
13. Pilyugin V.V., Milman I. Visual analytics and its use in the NRNU MEPhI "Scientific Visualization" laboratory activities. Scientific Visualization, Vol. 11, № 5, 2019, pp. 46–55 (doi:10.26583/sv.11.5.05) (http://sv-journal.org/2019-5/05/).
14. Kashevarova G.G., Martirosyan A.S., Travush V.I. Use of imaging in the forecasts of composite columns damage with stiff reinforcement. Scientific Visualization, Vol. 7, № 5, 2015, pp. 122–141 (http://sv-journal.org/2015-5/10.php?lang=en)
15. Van Dam, A., Forsberg, A. S., Laidlaw, D. H., LaViola, J. J., Simpson, R. M. Immersive VR for scientific visualization: A progress report. IEEE Computer Graphics and Applications, Vol. 20, № 6, 2000, pp. 26-52 (https://ieeexplore.ieee.org/abstract/document/888006)
16. Vinokur A.I., Kondratiev N.V., Ovechkis Yu.N. The research of the stereoscopic characteristics of virtual reality helmets // Scientific visualization, Vol. 12, № 1, 2020, pp. 61–69 (doi:10.26583/sv.12.1.05) (http://sv-journal.org/2020-1/05/?lang=en).
17. Semenov A. A. Strength and stability of geometrically nonlinear orthotropic shell structures // Thin-Walled Structures, Vol. 106, 2016, pp. 428–436, (doi:10.1016/j.tws.2016.05.018) (https://www.sciencedirect.com/science/article/abs/pii/S0263823116302816).
18. Aseev A.V., Makarov A.A., Semenov A.A.: Visualization of the stress-strain state of thin-walled ribbed shells. Bulletin of Civil Engineers, Vol. 3, 2013, pp. 226–232.